2018 IEEE Intelligent Vehicles Symposium (IV)
Changshu, Suzhou, China, June 26-30, 2018

Comparison of observers for vehicle yaw rate estimation

Nolwenn Monot, Xavier Moreau, André Benine-Neto, Audrey Rizzo, and François Aioun

***Abstract*— This paper presents a comparison of observers for vehicle lateral dynamics. Three model-based observers are compared: firstly Luenberger observer with a linear stationary model, secondly Kalman filter with a non stationary model and lastly Luenberger observers for each subsystems of a Takagi-Sugeno multi-model. Moreover, an analysis of the lateral dynamics shows that the model discretisation may be problematic according to the signal sampling theorem and a solution is proposed, such that all the observers can be used on board of the vehicle.**

I. INTRODUCTION

In the context of automated vehicle, the dynamic states of the vehicle need to be precisely known at every instant in order to perform the automated functions correctly. These states can either be measured using sensor or estimated using observation techniques. However, the more accurate a sensor is, the more expensive. Observers are then a good solution to improve a measurement of a less accurate sensor or to estimate the vehicle dynamics when there is no sensor.

The objective of this study is to improve the accuracy of the yaw rate sensor. There exist several methods in the literature to estimate the vehicle lateral dynamics. Usually, a bicycle model is used for the representation of the model as in [1] and [2]. The bicycle model is a physical representation of the vehicle dynamics, in [3] a comparison is made between the bicycle model and the kinematic model. Concerning the observation methods, a Luenberger observer (or gain matrix observer) is used in [2], Kalman filtering is preferred in [4] and [3], [5] choses a sliding mode observer and a fuzzy observer is used in [6].

The objective of this paper is to compare observers of the vehicle lateral dynamics for the estimation of the yaw rate. This observers include: a Luenberger observer with a simple linear stationary model of the vehicle, a Kalman filter and several Luenberger observers with a Takagi Sugeno multi-model. These observers are designed in order to be used with digital signals on board of the vehicle. It appears the sampling theorem is not verified at low speed, the paper also provides a solution for this problem.

The paper is organized as follows. Section II describes the vehicle lateral dynamics and an analysis in the frequency domain is made. Section III presents the different models, observers and combination used for the estimation of the system dynamics. Section IV introduces the problem with sampling for digital implementation of the observers at low longitudinal speed and proposes a solution. Section V presents a comparison of the observers with simulations.

N. Monot is with IMS Laboratory, Univ. Bordeaux, Bordeaux INP, CNRS, UMR 5218, 33405 Talence, France and also with Groupe PSA, 78943 Velizy-Villacoublay, France (e-mail: name.surname@mpsa.com).

X. Moreau and A. Benine-Neto are with IMS Laboratory, Univ. Bordeaux, Bordeaux INP, CNRS, UMR 5218, 33405 Talence, France (e-mail: name.surname@ims-bordeaux.fr).

A. Rizzo and F. Aioun are with Groupe PSA, 78943 Vélizy-Villacoublay, France (e-mail: name.surname@mpsa.com).

This work took place in the framework of the OpenLab 'Electronics and System for Automotive' combining IMS Laboratory and Groupe PSA company.

II. VEHICLE LATERAL DYNAMICS - FREQUENCY ANALYSIS

This section provides the equations of the vehicle lateral dynamics. These equations are then used in frequency domain to analyze the influence of the longitudinal speed on the vehicle lateral dynamics.

The dynamics are modelled using four-wheel representation of the vehicle with a symmetric distribution of the masses on the right and left wheelbases. The equations linked to the model and the linearization are explained in [7].

The state-space representation is defined using the signals of yaw rate ($\dot{\psi}(t)$), lateral speed ($v_y(t)$) and steering-wheel angle ($\theta_v(t)$):

$$\begin{cases} \dot{\underline{x}}(t) = A\underline{x}(t) + Bu(t) \\ y(t) = C\underline{x}(t), \end{cases} \tag{1}$$

with the state vector being $\underline{x}(t) = \begin{pmatrix} \dot{\psi}(t) \\ v_y(t) \end{pmatrix}$, the input control $u(t) = \theta_v(t)$ and the output $y(t) = \dot{\psi}(t)$.

All this signals can be seen on Fig. 1.

The matrices of the state-space representation (1) are:

$$A = \begin{bmatrix} -\dfrac{2(L_f^2 c_{yf} + L_r^2 c_{yr})}{I_z V_{x0}} & -\dfrac{2PDE}{I_z V_{x0}} \\ -\dfrac{2PDE}{M_t V_{x0}} - V_{x0} & -\dfrac{2(c_{yf} + c_{yr})}{M_t V_{x0}} \end{bmatrix},$$
$$B = \begin{bmatrix} \dfrac{2c_{yf} L_f}{\lambda I_z} \\ \dfrac{2c_{yf}}{\lambda M_t} \end{bmatrix} \text{ and } C = \begin{bmatrix} 1 & 0 \end{bmatrix}, \tag{2}$$

with $PDE = L_f c_{yf} - L_r c_{yr}$. All the parameters of the model are described in Table I.

The transfer function $G(s)$ of the state space representation (1) is computed with the relation:

$$G(s) = \frac{\dot{\Psi}(s)}{\Theta_v(s)} = C[sI - A]^{-1}B. \tag{3}$$

$G(s)$ can be written as a second order transfer function:

$$G(s) = K_0 \frac{1 + s/\omega_1}{1 + 2\zeta_0 s/\omega_0 + s^2/\omega_0^2}, \tag{4}$$

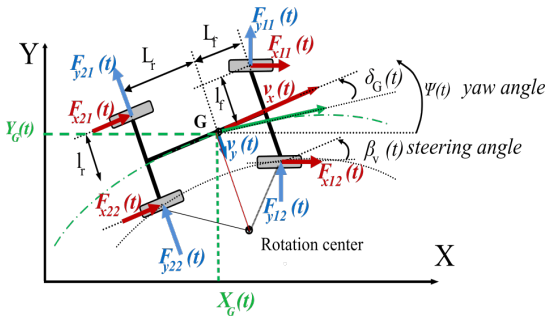

Fig. 1. Forces scheme

TABLE I
PARAMETERS OF THE DYNAMIC SYSTEM

V_{x0}	Longitudinal speed	Between 1 km/h and 130 km/h
μ	Road adhesion	1
M_t	Total mass of the vehicle	1759 kg
$M_{f/r}$	Front / rear mass	1319 kg / 439 kg
I_z	Moment of inertia	2638 kg.m^2
$L_{f/r}$	Front / rear wheelbase	0.71 m / 2.13 m
$c_{yf/r}$	Front / rear lateral cornering stiffness	94446 N.rad^{-1} / 48699 N.rad^{-1}
λ	Steering column gear rate	16

with coefficients that depend on the vehicle masses, the road adherence and the longitudinal speed such that:

$$\begin{aligned} K_0 &= \frac{2}{\lambda}\frac{c_{yf}c_{yr}LV_{x0}}{2c_{yf}c_{yr}L^2 - M_tV_{x0}^2PDE}, \\ \omega_0 &= \sqrt{2\frac{2c_{yf}c_{yr}L^2 - M_tV_{x0}^2PDE}{I_zM_tV_{x0}^2}}, \\ \zeta_0 &= \frac{I_z(c_{yf}+c_{yr}) + M_t(c_{yf}L_f^2 + c_{yr}L_r^2)}{\sqrt{2I_zM_t(2c_{yf}c_{yr}L^2 - 2M_tV_{x0}^2PDE)}} \\ \text{and } \omega_1 &= \frac{2c_{yr}L}{L_fM_tV_{x0}}. \end{aligned} \tag{5}$$

All these parameters, and so $G(s)$, are function of the longitudinal speed V_{x0}. The bode diagram of $G(s)$ for different speed V_{x0} is plotted on Fig. 2.

There is an important variation of the gain and the natural frequency in function of the longitudinal speed. All the coefficient of $G(s)$ are plotted on Fig. 3 and Fig. 4.

As it can be observed in these figures, as well as in the Bode diagram, the lower the speed, the greater the variation of K_0, ω_0 and ω_1.

III. Models and Observers

The design of an observer requires a model of the system. The choice of the observer is done in function of the available model. This section presents different representations of the vehicle lateral dynamics, several observers and the different combination between model and observer that are compared in section V.

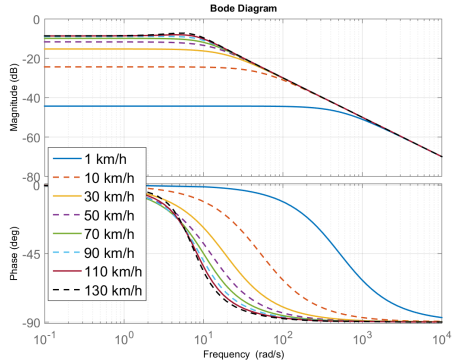

Fig. 2. Bode diagrams of $G(s)$

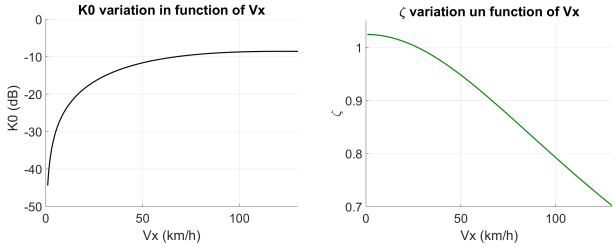

(a) (b)

Fig. 3. Variation of the gain K_0 (a) and the damping factor ζ (b) as a function of the longitudinal speed V_{x0}

A. Models

1) Linear model: The most common way to observe signals of a system is to use a linear model as in (1). With this model, the longitudinal speed is supposed to be fixed at $V_{x0} = 90$km/h.

2) Non stationary model: Because the longitudinal speed can vary through time, the state space representation (1) should be written as a non stationary model such that:

$$\begin{cases} \dot{\underline{x}}(t) = A(t)\underline{x}(t) + Bu(t) \\ y(t) = C\underline{x}(t), \end{cases} \tag{6}$$

with

$$A(t) = \begin{bmatrix} -\dfrac{2(L_f^2c_{yf} + L_r^2c_{yr})}{I_zV_x(t)} & -\dfrac{2PDE}{I_zV_x(t)} \\ -\dfrac{2PDE}{M_tV_x(t)} - V_x(t) & -\dfrac{2(c_{yf}+c_{yr})}{M_tV_x(t)} \end{bmatrix}. \tag{7}$$

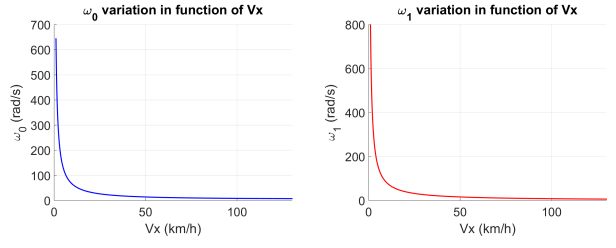

(a) (b)

Fig. 4. Variation of the frequencies ω_0 (a) and ω_1 (b) as a function of the longitudinal speed V_{x0}

3) Takagi-Sugeno model: is a non stationary model [8] such as (6) that has been linearized with a non-stationary parameter $\xi(t)$ using several subsystems. It is written:

$$\begin{cases} \dot{x}(t) = \sum_{i=1}^{r} \nu_i\left(\xi(t)\right)\Big(A_i x(t) + B_i u(t)\Big) \\ y(t) = \sum_{i=1}^{r} \nu_i\left(\xi(t)\right)\Big(C_i x(t) + D_i u(t)\Big), \end{cases} \tag{8}$$

with $\xi(t)$ the activation parameter, r the number of subsystems, ν_i the weight of the susbsystem i and (A_i, B_i, C_i, D_i) the matrices of each subsystem.

The non-stationary model of the vehicle lateral dynamics (6) depends on two non-stationary functions $f_1(V_x(t))$ and $f_2(V_x(t))$ such that:

$$\begin{cases} f_1(V_x(t)) = \dfrac{1}{V_x(t)} \\ f_2(V_x(t)) = V_x(t). \end{cases} \tag{9}$$

Since the speed varies in the range [1km/h; 130km/h], these functions are bounded and continuous and can be written:

$$\begin{cases} f_1(V_x(t)) = f^1_{min}\alpha^1_1(V_x(t)) + f^1_{max}\alpha^1_2(V_x(t)) \\ f_2(V_x(t)) = f^2_{min}\alpha^2_1(V_x(t)) + f^2_{max}\alpha^2_2(V_x(t)), \end{cases} \tag{10}$$

with α^j_1 and α^j_2 the local weights of f_j function.

The local weights can be expressed with the minimum and maximum values of the functions f_1 and f_2:

$$\begin{cases} \alpha^j_1(V_x(t)) = \dfrac{f^j_{max} - f_j(V_x(t))}{f^j_{max} - f^j_{min}} \\ \alpha^j_2(V_x(t)) = \dfrac{f_j(V_x(t)) - f^j_{min}}{f^j_{max} - f^j_{min}}. \end{cases} \tag{11}$$

Because there are two non-stationary functions, it leads to four subsystems and thus four A_i matrices:

$$A_1 = \begin{bmatrix} -\frac{2}{I_z} f^1_{max}(L_f^2 c_{yf} + L_r^2 c_{yr}) & \frac{-2}{I_z} f^1_{max} PDE \\ \frac{-2}{M_t} f^1_{max} PDE - f^2_{max} & \frac{-2}{M_t} f^1_{max} c_y \end{bmatrix}$$

$$A_2 = \begin{bmatrix} -\frac{2}{I_z} f^1_{max}(L_f^2 c_{yf} + L_r^2 c_{yr}) & \frac{-2}{I_z} f^1_{max} PDE \\ \frac{-2}{M_t} f^1_{max} PDE - f^2_{min} & \frac{-2}{M_t} f^1_{max} c_y \end{bmatrix}$$

$$A_3 = \begin{bmatrix} -\frac{2}{I_z} f^1_{min}(L_f^2 c_{yf} + L_r^2 c_{yr}) & \frac{-2}{I_z} f^1_{min} PDE \\ \frac{-2}{M_t} f^1_{min} PDE - f^2_{max} & \frac{-2}{M_t} f^1_{min} c_y \end{bmatrix}$$

$$A_4 = \begin{bmatrix} -\frac{2}{I_z} f^1_{min}(L_f^2 c_{yf} + L_r^2 c_{yr}) & \frac{-2}{I_z} f^1_{min} PDE \\ \frac{-2}{M_t} f^1_{min} PDE - f^2_{min} & \frac{-2}{M_t} f^1_{min} c_y \end{bmatrix}, \tag{12}$$

with $c_y = c_{yf} + c_{yr}$.

The subsystems are weighted by the global weights ν_i:

$$\begin{aligned} \nu_1(V_x(t)) &= \alpha^1_2(V_x(t))\alpha^2_2(V_x(t)) \\ \nu_2(V_x(t)) &= \alpha^1_2(V_x(t))\alpha^2_1(V_x(t)) \\ \nu_3(V_x(t)) &= \alpha^1_1(V_x(t))\alpha^2_2(V_x(t)) \\ \nu_4(V_x(t)) &= \alpha^1_1(V_x(t))\alpha^2_1(V_x(t)), \end{aligned} \tag{13}$$

so that (6) becomes:

$$\begin{cases} \dot{\underline{x}}(t) = \sum_{i=1}^{4} \nu_i\left(V_x(t)\right)\Big(A_i \underline{x}(t) + Bu(t)\Big) \\ y(t) = C\underline{x}(t). \end{cases} \tag{14}$$

B. Observers

1) Luenberger: A Luenberger observer [9] is an observer that can be used with linear system. It uses a gain matrix L to correct estimation with a measure such that:

$$\begin{cases} \dot{\hat{\underline{x}}}(t) = A\hat{\underline{x}}(t) + Bu(t) + L(y(t) - \hat{y}(t)) \\ \hat{y}(t) = C\hat{\underline{x}}(t). \end{cases} \tag{15}$$

The notations with a hat represent the estimated signals and those without a hat are the measured ones. L is the multiplying gain of the output error that enables to add a correction term in the state space representation (15). To keep the system stable, the eigenvalues of $(A - LC)$ should be negative. Moreover the other rule to respect, in order to have a faster convergence between the estimation and the measure, is the inequality $|eig(A - LC)| > |eig(A)|$.

2) Kalman filter: The Kalman filter [10] is an infinite impulse response filter that estimates the states of a system using a series of measurements. These measurements can be incomplete or contain noise. Because the Kalman filter will be used in the calculator on board of the vehicle with discrete signals, the discrete form of the Kalman filter is used. The discrete notation used in the following equations uses the subscript k for the instant k.

The state space representation (6) of the non-stationary model is discretized using the equations:

$$\begin{aligned} A_k &= e^{AT_s} \\ B_k &= A^{-1}(A_k - I)B, \end{aligned} \tag{16}$$

with T_s the sampling time. This discretization assumes there is a zero-order hold for the input and that A is nonsingular for every V_x.

The Kalman filter works in two steps: the prediction and the update. At a time k, knowing that $\hat{x}_{k|k}$ is the estimated state and $P_{k|k}$ is the error covariance matrix at k, the prediction step uses the estimate state of the previous sample to compute the estimation of the current state:

$$\begin{aligned} \hat{x}_{k|k-1} &= A_k \hat{x}_{k-1|k-1} + B_k u_k \\ P_{k|k-1} &= A_k P_{k-1|k-1} A_k^T + Q_k, \end{aligned} \tag{17}$$

with A_k the state transition matrix, B_k the matrix linking the control signals u to x, Q_k the covariance of the process noise, $\hat{x}_{k|k-1}$ the predicted state estimate and $P_{k|k-1}$ the a priori predicted estimate error covariance.

At the update step, the observations are used to correct the predicted state to obtain a more precise estimation:

$$\begin{aligned} \tilde{y}_k &= z_k - C\hat{x}_{k|k-1} \\ S_k &= CP_{k|k-1}C^T + R_k \\ K_k &= P_{k|k-1}C^T S_k^{-1} \\ \hat{x}_{k|k} &= \hat{x}_{k|k-1} + K_k \tilde{y}_k \\ P_{k|k} &= (I - K_k C)P_{k|k-1}, \end{aligned} \tag{18}$$

with z_k the measure, S_k the covariance of the update, R_k the noise covariance, K_k the Kalman gain and C is the same matrix as in (2).

C. Combination model/observer

Three combinations of model and observer have been introduced:

- Linear stationary model and Luenberger observer
- Linear non-stationary model and Kalman filter
- Takagi-Sugeno multi-model and 4 Luenberger observers, one for each subsystem.

Combining the Takagi-Sugeno multi-model with the Luenberger observer leads to the state-space representation:

$$\begin{cases} \dot{\underline{x}}(t) = \sum_{i=1}^{4} \nu_i\left(V_x(t)\right)\Big(A_i\underline{x}(t) + Bu(t) \\ \qquad\qquad + L_i(y(t) - \hat{y}(t))\Big) \\ y(t) = C\underline{x}(t). \end{cases} \tag{19}$$

IV. Sampling problem at low speed

In the calculators on board of the vehicle, the signals of the sensors are treated numerically at a discrete time of 40ms.

A. Signal sampling theorem

In order to estimate the vehicle yaw rate in discrete time on board of the vehicle, the signal sampling theorem needs to be verified. This theorem stipulates that a continuous time signal can be sampled when the sampling period f_s is greater or equal to two times the highest frequency component of the signal f_0. Knowing that for a frequency f, its corresponding angular frequency is $\omega = 2\pi f$, the theorem gives:

$$\omega_s \geq 2\omega_0, \tag{20}$$

with $\omega_s = 2\pi f_s$ the sampling frequency.

The sampling period is 0.04s, thus $\omega_s = 157\mathrm{rad/s}$. The signal sampling theorem is respected only if $\omega_0 < 78.5\mathrm{rad/s}$. However, for the considered system $G(s)$, the frequency ω_0 varies though time with the longitudinal speed V_x as it is shown with Fig. 4 (a). This figure shows that the theorem is not respected at low speed, when $V_x < 10\mathrm{km/h}$.

This should not be a problem for the combinations linear stationary model and Luenberger observer and linear non-stationary model and Kalman filter because for the first one, the model is linearized at $V_x = 90\mathrm{km/h}$ and for the second one, the assumption of a zero-order holder is made for the discretization in (16). A zero-order holder keeps constant the value of the sample u_k on all the interval $[k; k+1]$ enabling the attenuation of the unwanted frequencies superior to $\omega_s/2$. However, the Takagi-Sugeno model needs to be optimized to have a correct representation of the vehicle lateral dynamics at low speed.

B. Takagi-Sugeno model optimization

The estimation of the vehicle yaw rate is needed at all time, even when the speed is low. The idea to respect the sampling theorem at all speed is to optimize the global weights of the Takagi-Sugeno model in order to sufficiently decrease ω_0 but have a new gain as close as possible as K_0 in (5). To do that, at low speed when $V_x(t) < 20\mathrm{km/h}$, on the four weights $\nu_i(V_x(t))$ of the Takagi-Sugeno model, three are fixed and the last one is linear to $V_x(t)$ such that:

$$\begin{aligned} \nu_{1LS} &= \nu_1(20\mathrm{km/h}) \\ \nu_{2LS} &= \nu_2(20\mathrm{km/h}) \\ \nu_{3LS} &= \nu_3(20\mathrm{km/h}) \\ \nu_{4LS}(V_x(t)) &= aV_x(t) + b, \end{aligned} \tag{21}$$

with ν_{iLS} the global weights of the model at low speed and a and b, the coefficients that need to be found in order to obtain a model close to the reality that can be sampled.

With these weights, the parameters K_0 and ω_0 of the transfer function at low speed are:

$$\begin{aligned} K_{0LS} &= \frac{2c_{yf}c_{yr}L}{\lambda}\frac{\nu_{1LS} + \nu_{2LS} + \nu_{3LS} + aV_x + b}{2c_{yf}c_{yr}L^2\beta_1(V_x) - M_tPDE\beta_2(V_x)}, \\ \omega_{0LS}^2 &= \frac{2\beta_1(V_x)}{I_zM_t}\left(2c_{yf}c_{yr}L^2\beta_1(V_x) - M_tPDE\beta_2(V_x)\right) \\ &\text{with} \\ \beta_1(V_x) &= f_{max}^1(\nu_{1LS} + \nu_{2LS}) + f_{min}^1(\nu_{3LS} + aV_x + b) \\ \beta_2(V_x) &= f_{max}^2(\nu_{1LS} + \nu_{3LS}) + f_{min}^2(\nu_{2LS} + aV_x + b) \end{aligned} \tag{22}$$

The objective is to find a and b so that at all speeds:

- K_{0LS} is as close as possible to K_0,
- $\omega_{0LS} \leq 2\omega_s$,

To do that, the following cost function is minimized:

$$\begin{aligned} J(a,b) =& (K_{01} - K_{01LS})^2 + (K_{020} - K_{020LS})^2 + \\ & (2\omega_s - \omega_{01LS})^2 + (2\omega_s - \omega_{020LS})^2, \end{aligned} \tag{23}$$

where K_{0i} and K_{0iLS} are the gain K_0 and K_{0LS} at the speed i and ω_{0iLS} is the frequency ω_{0LS} at speed i.

This function takes into account the desired gain and frequency for the new parametrization of the model for the extreme speeds of the low speed interval in order to find a and b that match on all the low speed range.

The parameters a and b that minimizes the function J are computed using the gradient ∇J such that:

$$\nabla J(a,b) = \left[\frac{\partial J}{\partial a}\ \frac{\partial J}{\partial b}\right]'. \tag{24}$$

There are 5 solutions to the equation:

$$\nabla J(a,b) = [0\ 0]', \tag{25}$$

meaning that the pair (a, b) is an optimum of J.

To find if is these optimums are minimum or maximum, the hessian matrix $H(J)$ is computed:

$$H(J) = \begin{bmatrix} \frac{\partial^2 J}{\partial^2 a} & \frac{\partial^2 J}{\partial a \partial b} \\ \frac{\partial^2 J}{\partial b \partial a} & \frac{\partial^2 J}{\partial^2 b} \end{bmatrix} = \begin{bmatrix} r & v \\ v & w \end{bmatrix}. \tag{26}$$

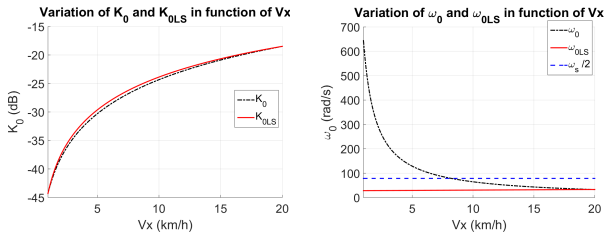

(a) (b)

Fig. 5. Variation of the gains K_0 and K_{0LS} (a) and the frequencies ω_0 and ω_{0LS} (b) as a function of the longitudinal speed V_{x0}

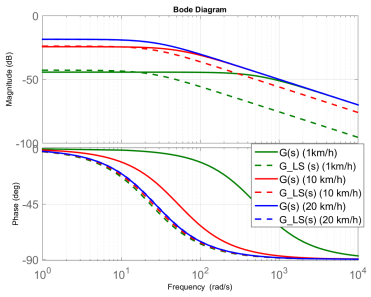

Fig. 6. Comparison of Bode diagrams of $G(s)$ and $G_{LS}(s)$

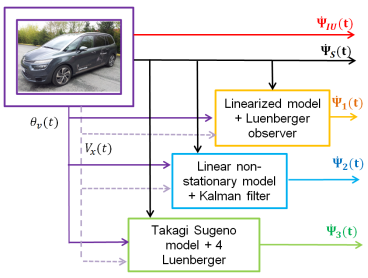

Fig. 7. Schematisation of the simulation

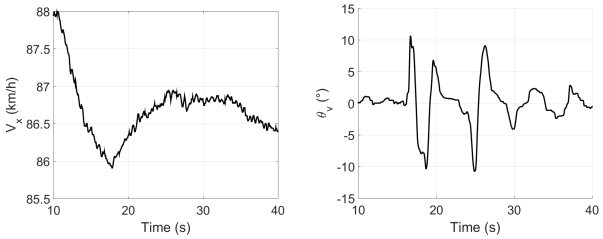

(a) (b)

Fig. 8. Evolution of the longitudinal speed $V_x(t)$ (a) and the steering wheel angle $\theta_v(t)$ (b) through time for high speed logged data

Depending on r, v and w, the pair (a, b) solution of (25) is:

- a minimum, if $rw - v^2 > 0$ and $r > 0$: (a, b),
- a maximum, if $rw - v^2 > 0$ and $r < 0$: (a, b),
- no statement can be made otherwise.

This method enables to find the local minimum and maximum. Three out of five solutions of (25) respect the conditions $rw - v^2 > 0$ and $r > 0$. The global minimum is computed numerically, resulting in $(a, b) = (0.1834, -0.1897)$.

The transfer function of the system (14) with $\nu_i = \nu_{iLS}$ is written $G_{LS}(s)$. The variation of the gain and the frequency of $G(s)$ and $G_{LS}(s)$ at low speed are compared on Fig. 5. As it can be seen on Fig. 5 (a), the gain of the optimized system at low speed is very close to the real one (maximum error of 8%). Concerning the frequency on Fig. 5 (b), ω_{0LS} is indeed inferior to $\omega_s/2$, meaning that the system, with this representation, can now be sampled. The Bode diagrams of the two transfer functions are plotted on Fig. 6 for 1km/h, 10km/h and 20km/h.

V. Simulation with real embedded data

The three observers described in section III.C are now compared using signals recording on an automated vehicle prototype. This prototype is a C4 Picasso from the AVA (Autonomous Vehicle for All) project of the Groupe PSA. Yaw rate sensors, which currently equip commercialized vehicles, have been mainly designed for ESP purposes and present poor measurements (dead-band) for low yaw rates. In order to design automated vehicle functionalities, accurate information on the yaw rate is required. It is there preferable to design observers than to design new sensors, which would certainly yield higher cost.

The sensor signals used in the following simulation are: the longitudinal speed V_x, the steering-wheel angle θ_v, the yaw rate measured directly by a currently-in-production sensor $\dot{\psi}_s$ and the yaw rate measured using an inertial unit $\dot{\psi}_{IU}$, which is used as the reference signal. The output of each observer is respectively $\dot{\psi}_1(t)$, $\dot{\psi}_2(t)$ and $\dot{\psi}_3(t)$, for the stationary model and Luenberger observer, the non-stationay model and Kalman filter and the Takagi-Sugeno model and 4 Luenberger observers. The scheme of the simulation is presented in Fig. 7.

Two simulations has been made, the first with logged data at high speed and the second with logged data at low speed.

A. High speed simulation

The input signals $V_x(t)$ and $\theta_v(t)$ of the observers for the first simulation are plotted on Fig.8 (a) and (b) respectively.

In this log, the longitudinal speed is close to 90km/h, which provides a fair comparison between the three observers because for this speed, all the models should be closed to the real system. The outputs and measured signals of the yaw rate are plotted on Fig. 9.

The inertial unit measured signal $\dot{\psi}_{IU}(t)$, plotted here in red. The yaw rate sensor measured signal $\dot{\psi}_S(t)$ is plotted in

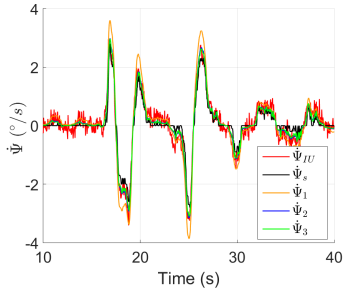

Fig. 9. Evolution of the measured and estimated yaw rate signals through time for high speed logged data

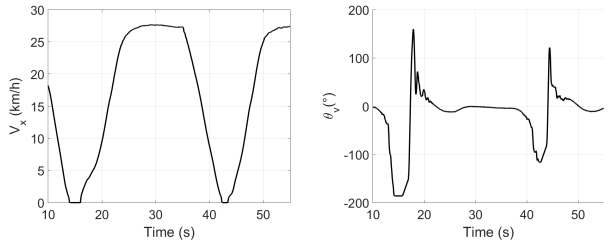

(a) (b)

Fig. 10. Evolution of the longitudinal speed $V_x(t)$ (a) and the steering wheel angle $\theta_v(t)$ (b) through time for low speed logged data

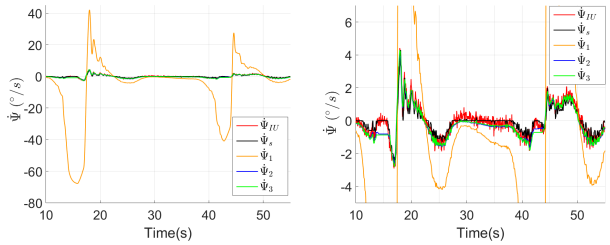

(a) (b)

Fig. 11. Evolution of the measured and estimated yaw rate signals through time for low speed logged data (a) and a zoom (b)

black. As stated, the sensor performs poorly around $0°/s$. It can be seen that sometimes, it does not provide information around this value.

When the steering wheel angle is small, $\theta_v(t) < 5°$, at the end of the log, all the observers manages to follow correctly the reference signal, even when the measure of the yaw rate used by the observers is not satisfactory. However, for higher steering wheel angle, the linearized model with one Luenberger observer does not manage to represent the dynamics correctly. The Kalman filter and the 4 Luenberger rather yield the same observation of $\dot{\psi}(t)$.

B. Low speed simulation

For this simulation, a log with very low speed has been tested. The first objective is to verify if the linear model at 90km/h can observe the vehicle lateral dynamics at speeds away from its original operating point, the second is to check if the zero-order holder included in the discretized representation of the model used for the Kalman filter is indeed able to reduce the frequency superior to $\omega_s/2$ at low speed and the last is to confirm that the Takagi-Sugeno model optimization is conform to the real lateral vehicle dynamics at speeds inferior to 20km/h.

The input signals $V_x(t)$ and $\theta_v(t)$ of the observers for the first simulation are plotted on Fig.10 (a) and (b) respectively. In this log, there are two regions around 15s and 43s where $V_x < 10$km/h and the models of the system can be possibly unrepresentative to reality. Because the speed is smaller, the steering wheel angle needed for a turn or a lane change is higher as at can be seen on Fig. 10 (b).

The outputs and measured signals of the yaw rate are plotted on Fig. 11. As expected, the model linearized at 90km/h is not representative of the vehicle lateral dynamics when the speed is not close to 90km/h. However, as for the high speed simulation, the two other combinations model/observer enable a good estimation of the yaw rate meaning the discretization (16) and the optimization of the Takagi-Sugeno model allow to overcome the problem of the signal sampling theorem at low speed.

This two methods have very similar results in simulation. The difference is the way to treat the model. The Kalman filter needs the discrete time matrices representing the system. At each sampling the matrix A_k needs to be nonsingular and matrix inversion calculation are made. The Takagi-Sugeno model needs less calculation on board of the vehicle, once it has been optimized. However, the optimization requires an important preliminary analysis of the system dynamics.

VI. CONCLUSIONS

Three different methods have been developed to observe the vehicle yaw rate. Because the lateral dynamics is strongly linked to the longitudinal speed that can vary through time, the simple method like linearization at a specific operating points is not efficient. The other two methods have similar output but are very different in the methodology. The Kalman filtering is easier to set up but needs the matrix of the state-space representation to be nonsingular at each time. The Takagi-Sugeno model that is coupled with Luenberger observers cannot be sampled as it is at low speed because the sampling theorem is not verify. The paper presented a method that solves the sampling problem by an optimization of the weights of the Takagi-Sugeno model. This optimization is more complex in term of calculation but guarantees a good modelling of the non stationary vehicle lateral model at every sample. Moreover the computation of the Luenberger observers is simple.

REFERENCES

[1] A. El Hajjaji, M. Chadli, M. Oudghiri, and O. Pages, "Observer-based robust fuzzy control for vehicle lateral dynamics," in *American Control Conference, 2006*, pp. 6–pp, IEEE, 2006.

[2] U. Kiencke and A. Daiß, "Observation of lateral vehicle dynamics," *Control Engineering Practice*, vol. 5, no. 8, pp. 1145–1150, 1997.

[3] J. Farrelly and P. Wellstead, "Estimation of vehicle lateral velocity," in *Control Applications, 1996., Proceedings of the 1996 IEEE International Conference on*, pp. 552–557, IEEE, 1996.

[4] L. Chu, Y. Zhang, Y. Shi, M. Xu, and M. Liu, "Vehicle lateral and longitudinal velocity estimation based on unscented kalman filter," in *Education Technology and Computer (ICETC), 2010 2nd International Conference on*, vol. 3, pp. V3–427, IEEE, 2010.

[5] J. Stéphant, A. Charara, and D. Meizel, "Evaluation of a sliding mode observer for vehicle sideslip angle," *Control Engineering Practice*, vol. 15, no. 7, pp. 803–812, 2007.

[6] M. Oudghiri, M. Chadli, and A. El Hajjaji, "Lateral vehicle velocity estimation using fuzzy sliding mode observer," in *Control & Automation, 2007. MED'07. Mediterranean Conference on*, pp. 1–6, IEEE, 2007.

[7] N. Monot, X. Moreau, A. Benine-Neto, A. Rizzo, and F. Aioun, "Dynamic stability control system: the crone approach," *IFAC-PapersOnLine*, vol. 50, no. 1, pp. 13822–13827, 2017.

[8] T. Takagi and M. Sugeno, "Fuzzy identification of systems and its applications to modeling and control," *IEEE transactions on systems, man, and cybernetics*, no. 1, pp. 116–132, 1985.

[9] D. Luenberger, "An introduction to observer," *IEEE Transactions on automatic control*, vol. 16, no. 6, pp. 596–602, 1971.

[10] R. E. Kalman *et al.*, "A new approach to linear filtering and prediction problems," *Journal of basic Engineering*, vol. 82, no. 1, pp. 35–45, 1960.